This is an open access article published under an ACS AuthorChoice License, which permits copying and redistribution of the article or any adaptations for non-commercial purposes.

Macromolecules

Article

pubs.acs.org/Macromolecules

The Polyelectrolyte Complex/Coacervate Continuum

Qifeng Wang and Joseph B. Schlenoff*

Department of Chemistry and Biochemistry, The Florida State University, Tallahassee, Florida 32306, United States

Supporting Information

ABSTRACT: Stoichiometric polyelectrolyte complexes (PECs) of the strong polyelectrolytes poly(styrenesulfonate) (PSS) and poly(diallyldimethylammonium) (PDADMA) were dissociated and dissolved in aqueous KBr. Water was added to dilute the salt, allowing polyelectrolytes to reassociate. After appropriate equilibration, these mixtures yielded compositions spanning complexes (solid) to coacervates (elastic liquid) to dissolved solutions with increasing [KBr]. These compositions were defined by a ternary polymer/water/salt phase diagram. For coacervates, transient microphase separation could be induced by a small departure from equilibration temperature. A boundary between complex and coacervate states was defined by the crossover point between loss and storage modulus. Salt ions within the complex/coacervate were identified as either ion paired with polyelectrolytes ("doping") or unassociated. The fraction of ion pair cross-links between polyelectrolytes as a function of KBr concentration was used to account for viscosity using a model of "sticky" reptation.

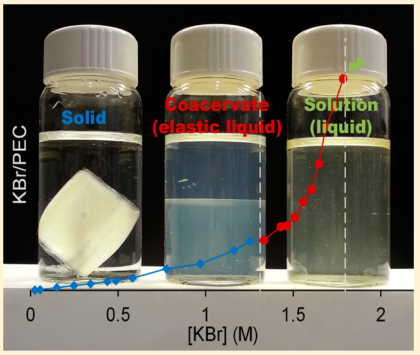

INTRODUCTION

Oppositely charged macromolecules condense from solution to yield an interesting range of soft matter.[1,2] Synthetic polyelectrolytes rely mainly on ion pairing between opposite charges to associate, whereas biopolymers often have additional driving forces, such as hydrogen bonding and hydrophobic forces, at their disposal.[3,4]

Morphologies of associated polyelectrolytes differ widely, depending on the balance of water, polymer and salt ions within the complex.[5] Research on associated polyelectrolytes has historically focused on two, loosely defined morphologies. To make so-called "polyelectrolyte complexes," PECOX, solutions of polyanions and polycations are typically mixed to yield dense precipitates.[6−9] Once entrained water is removed,[5] the wet complexes are stiff or rubbery, depending on their salt content.[2] Their proposed applications stem from their solid-like properties. In contrast, "polyelectrolyte coacervates," PECOV, also called "polyelectrolyte complex coacervates," are loosely associated polyelectrolytes with more liquid-like properties.[10−12] Interestingly, research on these two morphologies of associated polyelectrolytes has followed parallel but distinct paths with little effort to probe the commonalities between them.

The term "coacervate" is broadly used to describe a phase-separated solution mixture where there are at least two phases: one rich and one poor in a particular component.[13−15] The polyelectrolyte complex coacervate was so-named by Bungenberg de Jong and Kruyt to distinguish coacervation between two polyelectrolytes from that between a polyelectrolyte and a small molecule or colloid.[16] Interest in polyelectrolyte complex coacervates has recently been stimulated by the finding that they are produced by natural organisms such as tubeworms, mussels, and sandcastle worms.[4,17] For example, the sandcastle worm bonds sand and seashell hash together with coacervate for physical protection.[17] Biomedical applications for coacervates include deep tissue bonding or bone fixation,[18] scaffold coatings,[19] bone cement,[4,18] membrane-free protocell models,[20,21] and drug encapsulating materials.[22]

Interest in polyelectrolyte complexes was boosted with the introduction of synthetic polymers.[23] Michaels et al. were pioneers in the early exploration of the properties of PECs, showing the interplay between salt concentration, organic modifier and polymer concentration in ternary phase diagrams.[2,24] Proposed applications[2] included membranes for ultrafiltration, battery and fuel cell separators, conductive coatings, medical implants and contact lenses, and chemical sensors. Unlike coacervates, polyelectrolyte complexes were shown to be intractable, as they could not be melted or processed in solid form.[1,2,24] PECOXs bore the stigma of being "unprocessable" until the Decher group introduced the modern era of layer-by-layer deposition of polyelectrolytes, yielding a plethora of new applications for PECOX in ultrathin film morphology.[25−27] Our recent finding that PECOX may be extruded into large articles if sufficiently plasticized with salt and water ("saloplasticity") has introduced yet another processing dimension.[28,29]

Because the composition of PECOXs from synthetic polyelectrolytes is defined and controlled they are now understood quite well, unlike coacervates, perhaps because some of the better studied coacervates include intricate biopolymers such as proteins.[10,22,30−32] It is now known that all of the properties of PECOX in contact with aqueous

Received: March 10, 2014
Revised: April 21, 2014
Published: April 28, 2014

 © 2014 American Chemical Society dx.doi.org/10.1021/ma500500q | Macromolecules 2014, 47, 3108−3116

solutions are controlled by their salt and water content. The fundamental unit of interaction in a PEC is the ion pair Pol^+Pol^- between two charged monomer units. These interactions are broken with the addition of salt, transforming "intrinsic" charge compensation to "extrinsic", where polyelectrolyte segments are paired with, and compensated by, salt counterions, M^+ and A^-.[28,33,34]

$$Pol^+Pol^- + M_{aq}^{\ +} + A_{aq}^{\ -} \leftrightharpoons Pol^+A^- + Pol^-M^+ \quad (1)$$

The "doping level," y, is the fraction of polyelectrolyte compensated by counterions:

$$y = \frac{[Pol^+A^-]}{[Pol^+Pol^-] + [Pol^+A^-]} \quad (2)$$

recognizing that $[Pol^+A^-] = [Pol^-M^+]$. A nice example of salt-controlled properties in PECOX is the strong dependence of bulk modulus on the density of Pol^+Pol^- pairs,[35] since they are physical cross-links which can be broken by salt.

Pressing the salt "doping" represented in eq 1 to the extreme breaks more and more ion pairs and eventually dissociates polyelectrolyte chains from each other completely.[36−38] Just before this critical dissociation point, polyelectrolytes should be associated extremely loosely. The purpose of this work is to probe the properties of these weakly associated PECs, which are, in fact, coacervates and, with salt, connect the entire spectrum of the same associated polyelectrolytes from complex to coacervates. An attempt is made to define a boundary between the two states using both composition and properties.

EXPERIMENTAL METHODS

Materials. Poly(4-styrenesulfonic acid, sodium salt) (AkzoNobel, VERSA TL130, molar mass ca. 200 000 g mol^{-1}) and poly(diallyldimethylammonium chloride) (Ondeo-Nalco, SD 46104, molar mass ca. 400 000 g mol^{-1}) were used as received. All salt solutions were prepared using deionized water (18 MΩ Barnstead, E-pure).

Stoichiometric PECs. Individual solutions of PSSNa and PDADMAC were prepared at a concentration of 0.125 M with respect to their monomer units and neutralized with a few drops of 0.1 M NaOH or HCl. The concentration of salt in these solutions was adjusted to 0.25 M by adding NaCl. PEC was precipitated by simultaneously mixing stoichiometric amounts of both solutions in a large beaker under stirring.[28] After being stirred for 30 min, the precipitate was decanted, rinsed in 1.0 M NaCl, and chopped into ca. 1 cm pieces. PEC pieces were soaked in water, which was changed every 12 h until the electrical conductivity of the water rinse fell below 3 μS cm^{-1}. Complete removal of salt by rinsing thus has been proven in previous work using (radioactive) $^{22}Na^+$.[39] The PEC was dried for ca. 24 h at 120 °C to constant weight. Finally, the dry PEC was ground into a powder and stored in a desiccator. Coacervate samples were typically prepared by dissolving 1.50 g of the PEC powder in V_1 mL of 2.50 M KBr solution (Table 1). After the PEC was completely dissolved, V_2 mL of water (Table 1) was added to the PEC/KBr solution dropwise with vigorous stirring. Here $V_1 + V_2 = 15$ mL. The final concentration of PEC and KBr was measured after two stable phases had formed. This process, termed the "backwards" method (since we start with a solution of dissolved PEC and dilute to decrease [salt]), speeds the preparation of coacervates, especially those having relatively low [KBr].

Methods and Equipment. To determine the polymer and salt content of the PECs, thermal gravimetric analysis (TGA) was performed with a SDT Q600 TGA from TA Instruments with a heating rate of 20 °C min^{-1} from room temperature to 100 °C, isothermal at 100 °C for 60 min to remove most of water in the samples, followed by a heating rate of 10 °C min^{-1} from 100 to 700 °C. Mechanical analysis was performed with a temperature-controlled

Table 1. Components of Each Vial in Figure 1 and Corresponding KBr Concentration

samples[a]	PEC[b] (g)	2.5 M KBr (mL)	H_2O (mL)	[KBr][c] (M)
$PEC_{1.33}$	1.5	8.4	6.6	1.33
$PEC_{1.43}$	1.5	9.0	6.0	1.43
$PEC_{1.46}$	1.5	9.3	5.7	1.46
$PEC_{1.51}$	1.5	9.6	5.4	1.51
$PEC_{1.56}$	1.5	9.9	5.1	1.56
$PEC_{1.60}$	1.5	10.2	4.8	1.60
$PEC_{1.65}$	1.5	10.5	4.5	1.65
$PEC_{1.69}$	1.5	10.8	4.2	1.69
$PEC_{1.73}$	1.5	11.1	3.9	1.73
$PEC_{1.78}$	1.5	11.4	3.6	1.78
$PEC_{1.84}$	1.5	11.7	3.3	1.84
$PEC_{1.88}$	1.5	12.0	3.0	1.88

[a]The [KBr] are shown by subscripts. [b]Dry, salt-free, stoichiometric. [c][KBr] listed here is [KBr] in the dilute phase.

RheoStress 300 rheometer in a cone/plate (C35/2Ti titanium plate with 2° cone and a diameter of 35 mm) or a parallel plate (type PP20 stainless steel plate with a diameter of 20 mm) configuration. The surface of the parallel plate was roughened by sandblasting to minimize sample slip (roughness ca. 15 μm). Gel-like samples were compressed by 15%, and dynamic oscillatory shear experiments were carried out with the temperature set to 20.0 ± 0.1 °C and an oscillating shear stress of 25 Pa over the frequency range 0.1−100 Hz for samples with different KBr concentration. Other parameters were: 300 s thermal equilibrium, 1 s delay time, and six measurements for each data point. The above parameters allowed the measurement of the storage modulus (G'), the loss modulus (G''), and viscosity, η.

KBr concentrations in dilute phase and uniform solution were also measured precisely by conductivity. The samples for conductivity were prepared by mixing 50 μL dilute phase solution (or uniform solution) in 15 mL water for at least 24 h making sure the KBr was completely released. The conductivity was measured in a thermostated cell at 25.0 ± 0.1 °C equipped with a stir bar and a four-probe conductivity electrode (Orion 3 Star, Thermo Scientific). The conductivity was recorded every 30 s until it reached a plateau. A standard curve of [KBr] was used to convert conductivity to concentration.

Homogeneous fiber samples for PECOX doping were prepared by extrusion.[28] After two consecutive extrusions, the stoichiometric (1:1 PSS:PDADMA) extruded PECs (exPECs) were annealed in 1.5 M NaCl for 24 h, then soaked in excess water to remove all ions. The exPEC rods were cut into samples approximately 2 cm long, dabbed dry with a paper wipe and immersed separately into solutions of various KBr concentrations. Each sample was allowed to dope to equilibrium at room temperature (23 ± 2 °C) for at least 24 h. PECs were wiped then dropped into 50 mL of water to release the salt. Plateau conductivity values of the water were translated to the amount of KBr released. After complete release of salt, exPECs were dried at 120 °C for 6 h to obtain the dry mass of the complex.

Proton NMR spectroscopy (Bruker Avance 600 MHz spectrometer) was used to measure the ratio of PSS to PDADMA in the PEC coacervate as follows: diluted or concentrated phase of coacervate samples containing ca. 30 mg PEC were dried at 120 °C to remove water completely. The dried, KBr-loaded samples were then dissolved in 0.8 mL D_2O or 2.5 M KBr in D_2O. In some samples, additional D_2O was needed to dissolve all KBr. For calibration, spectra of mixtures of known amounts of PSS and PDADMA in 2.5 M KBr were recorded under the same conditions.

For imaging, coacervate samples were sealed between a coverslip and a microscope slide and imaged with a Nikon Eclipse Ti inverted microscope fitted with a Photometrics Cool Snap HQ2 camera and NIS Elements AR 3.0 software. Differential interference contrast (DIC) images with magnification 100× or 200× were obtained. Fluorescence images were acquired using excitation at 450−490 nm and emission at 500−550 nm. Turbidities at 500 nm of both dilute and

dx.doi.org/10.1021/ma500500q | Macromolecules 2014, 47, 3108−3116

concentrated phases of coacervate samples were measured with a Cary 100 Bio UV–vis spectrometer with temperature control. A heating/cooling ramp of 0.1 °C min^{-1} was used.

RESULTS AND DISCUSSION

While precipitates from PSS and PDADMAC had the typical "cottage cheese curd" consistency of many PECOX, the extruded forms were tough and dense, with modulii approaching 15 MPa when wet.[28] The starting material for coacervates was stoichiometric, dry powdered complex. Residual NaCl was washed out of this material before use. In the present work, material properties were always measured with the PECOX or PECOV in contact with salt solution, ensuring equilibrium contents of water and salt, both vital to the properties.[40] The term PEC is used herein to refer to all of the components of associated, hydrated polyelectrolyte complexes, whether in PECOX or PECOV morphology. The term PE refers to the polyelectrolyte constituents only.

An increase in salt concentration leads to an increase in salt and water content in the PEC. At the same time, polymer ion pairs are broken. The overall transformation is depicted in Scheme 1, starting with the undoped PEC immersed in water.

Scheme 1. Illustration of the Effect of Added Salt (Increasing from Left to Right) on the Microstructures of PEC Solid (Undoped), Solid (Doped), Coacervate, and Solution[a]

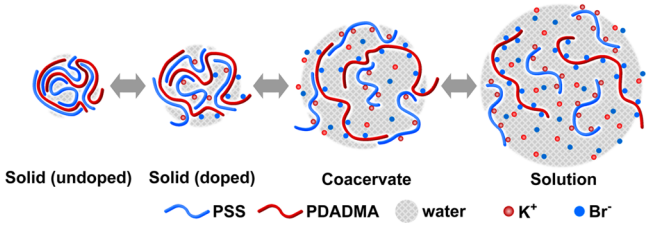

[a]All steps are reversible and all compositions are in equilibrium.

The undoped PEC has no salt ions and about 38 wt % water, which represents about ten water molecules hydrating each Pol^+Pol^- ion pair.[28] Salt added to solution promotes doping of ions into the PEC (eq 1), bringing in additional water. At this point, each salt ion pairs with a polyelectrolyte segment, breaking an ion pair. At higher salt concentration the density of cross-linking becomes much lower and some of the ions in the PEC are not associated specifically with polyelectrolyte. In the final step, every polymer/polymer ion pair is broken, the chains dissociate, and the PEC dissolves.

In this research, the chaotropic salt KBr was used to dope PEC. KBr has a higher doping constant compared to NaCl. With a diffusion coefficient of about 10^{-6} cm^2 s^{-1} it would take on the order of an hour to reach doping equilibrium for a 1 mm diameter PEC fiber in [KBr] < 1.3 M,[39] whereas it would take days to weeks to achieve a stable coacervate composition starting with dry PEC. As an alternative to adding the desired salt concentration to reach the final complex or coacervate composition, sufficient KBr was added to completely dissolve the PEC, then water was added to the solution to dilute the salt to a final concentration. This "backwards" method more rapidly provided (apparently) equilibrated PEC than the "forwards" method (see Supporting Information, Figure S1). In a final treatment aimed at obtaining truly equilibrium compositions, samples were warmed at 60 °C for 3 h then allowed to stabilize at room temperature for several days.

Figure 1 shows the appearance of equilibrated materials starting with a constant amount of salt-free dry PEC. The addition of 2.5 M KBr dissolved the PEC. The final salt concentration was then set by the addition of various volumes of water, listed in Table 1. After "annealing" at 60 °C and cooling to room temperature a clear range of phase separation behaviors was observed. PEC at lower salt concentrations took on the appearance of solid PECOX equilibrated in salt, being rather opaque and having the consistency of an extremely soft rubber. Additional KBr led to a significant increase in the PEC volume, whereupon the condensed or polymer-rich phase became clear and took on the fluid consistency of a PECOV. The ratio of the polymer-rich to polymer-poor phase increased until, at about 1.80 M KBr, a single phase was achieved.

In all cases, near-equilibrium conditions were demonstrated by the fact that the compositions were almost the same whether approached in the "forward" or "backward" direction. In addition, at equilibrium, viscosity, which is highly sensitive to composition (see below) remained constant. Phase separation occurred at room temperature from sample $PEC_{1.33}$ to $PEC_{1.69}$ (subscripts show the [KBr] in the dilute phase). Clearly developed phase boundaries took longer for samples with lower [KBr] (e.g., several weeks for $PEC_{1.33}$ and only about 2 days for $PEC_{1.69}$) due to higher viscosities of the coacervate phases at lower [KBr]. Phase separation of $PEC_{1.73}$ and $PEC_{1.78}$ was observed only after annealing at higher temperatures and cooling back down to room temperature.

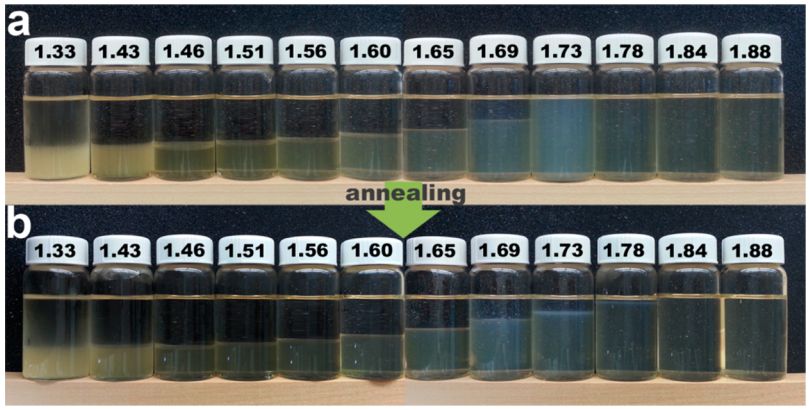

Figure 1. Photos of (a) as-prepared PSS/PDADMA coacervate samples (< 1.80 M KBr) and uniform solutions (> 1.80 M KBr) stored for 30 days and (b) the samples 10 days after annealing for about 3 h at 60 °C and cooled to room temperature. The numbers are the [KBr] of each sample.

dx.doi.org/10.1021/ma500500q | Macromolecules 2014, 47, 3108–3116

Qualitatively, it can be concluded that a wide variety of PEC phase space may be accessed simply by the addition of a salt, as has been known for many decades.[6] The only point which can be labeled an actual phase transition is the dissolution point. In truly dissolved PECs the individual polymer chains are probably separated from each other, which requires high salt concentrations. The critical salt concentration for dissolution, $[salt]_c$, depends on a number of factors, but mainly on the identity of the polyelectrolyte pair, the salt type, and the solvent. Specifically, PECs which are more easily doped (eq 1), and salts which more effectively dope (ranked according to the Hofmeister series[41]), have a lower $[salt]_c$. Less commonly, an organic modifier may be added to enhance doping by a particular salt. Michaels described such ternary solvents to produce solutions of dissolved PEC.[2,24] In the present case, the choice of PSS and PDADMA yields the PECOX → PECOV → solution spectrum of behaviors with an appropriately "strong" doping salt such as KBr without recourse to organic modifiers. An essential feature of KBr is that it does not precipitate either individual PSS or PDADMA components up to the concentrations used here.

Phase separation for the solid PECOX is less intriguing than for the liquid-like PECOV. In fact, the liquid-like properties of coacervates can facilitate handling on a large scale.[3,10] Phase separations are observed on two scales: macrophase separation is represented by the two clearly demarcated phases as seen in Figure 1 ($PEC_{1.33}$–$PEC_{1.78}$). Microphase separation is revealed by turbidity in either of the two macrophases. For the present combination of polyelectrolytes, it turns out that most compositions of PECOVS are on the verge of microphase separation, which is seen as microscopic droplets in a continuous background.

Microphase separation is induced by changing the temperature away from the equilibration temperature. An example is shown in Figure 2 which depicts micrographs of the two

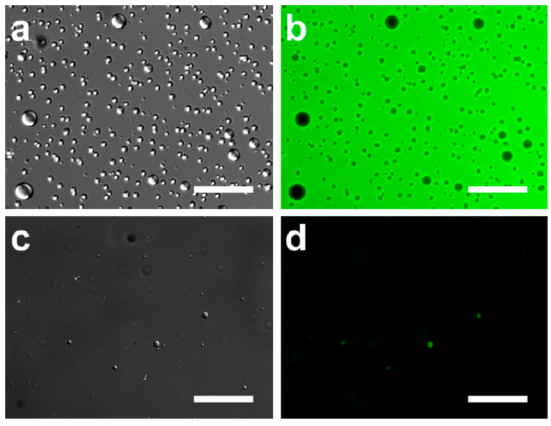

Figure 2. Microphase separation of $PEC_{1.69}$ shown by microscopy in DIC (left) and fluorescence (right) modes of coacervate phase (a, b) and dilute phase (c, d), taken above the equilibration temperature (room temperature). Scale bars are 100 μm.

macrophases from $PEC_{1.69}$. As soon as the temperature is raised a few degrees (by the lamp illuminating the sample) microphase droplets appear in both phases. Exploiting the (weak) fluorescence of the PSS component, it is seen that, on heating, the PE-rich macrophase contains PE-poor microdroplets (the fluorescence is lower) and the PE-poor macrophase contains PE-rich microdroplets. This means the binodal shifts to a more concentrated coacervate phase and a more dilute dilute phase.

To better control the temperature, turbidimetry was performed on both macrophases using a UV–vis spectrometer. For a sample equilibrated at room temperature (23 ± 2 °C) Figure 3 shows that both macrophases undergo microphase

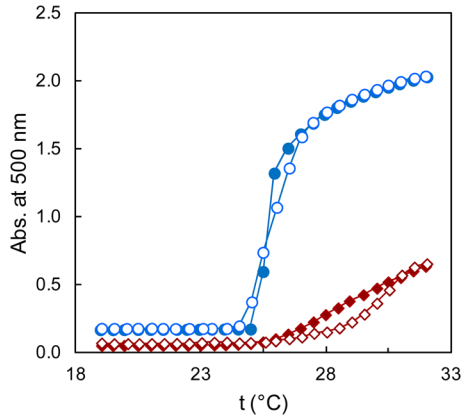

Figure 3. Turbidity versus temperature of coacervate (blue circles) and dilute (red diamonds) phases of $PEC_{1.69}$. Solid and empty symbols are for heating and cooling, respectively. The heating/cooling rate was 0.1 °C min^{-1}.

separation (becoming turbid) on warming. This phase separation is reversible, with low hysteresis, if the temperature ramp is performed slowly.

For the PSS/PDADMA coacervate studied here, microphase separation is a nonequilibrium condition. Imaging of the microphase separation following an increase in temperature showed that the droplets coalesced with time and eventually the macrophase clarified at a new equilibrium composition. A video demonstrating droplet coalescence is provided in Supporting Information. For most of the [KBr], microphase separation was induced by a slight perturbation of the temperature away from the equilibration temperature. Following a temperature increase of a few degrees, microphase separation spread out from the interface into both dilute and coacervate phases. Figure 4 shows the band of temperatures over which microphase separation was observed. As $[KBr]_c$ is approached the macrophases swiftly become much more temperature stable. When the [KBr] is

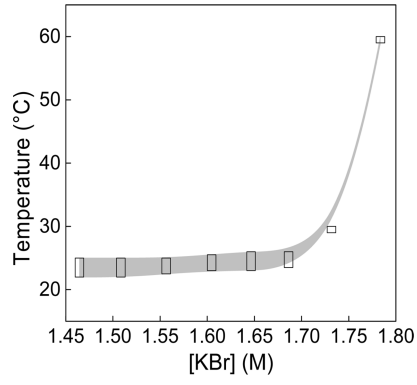

Figure 4. Temperature range for microphase separation of coacervate samples equilibrated at room temperature. The float bars and gray area show the approximate temperature where the microphase separation starts at the interface and spreads throughout the coacervate.

dx.doi.org/10.1021/ma500500q | Macromolecules 2014, 47, 3108–3116

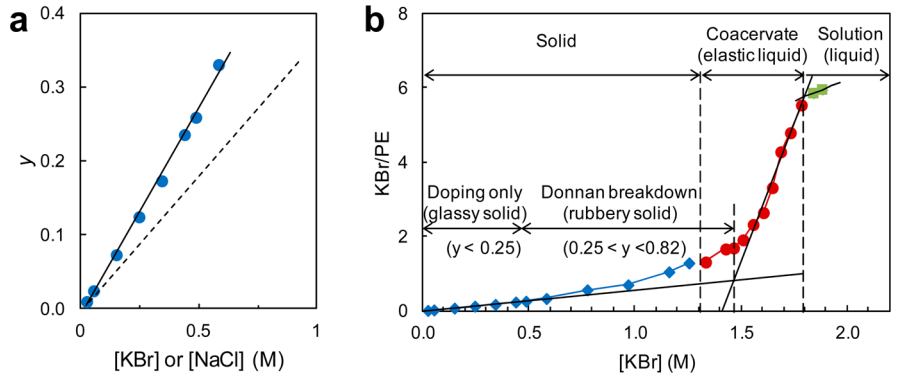

Figure 5. (a) Linear dependence of KBr/PE (blue circles) on [KBr] for doping of PSS/PDADMA, where doping level, y, = KBr/PE (for [KBr] < 0.6 M). The doping of PSS/PDADMA by NaCl is shown by dotted line, taken from ref 39. (b) KBr/PE in PECOX form (blue diamonds) and as PECOV (red circles) and uniform solution, where the PEC is dissolved (green squares). When the linear doping regime is extrapolated to y = 1.00, the [KBr] = 1.80 M. Boundaries between glassy, rubbery, and elastic liquid states are not sharp.

higher than $[KBr]_c$, no phase separation can be observed, even if solutions are heated above 80 °C.

The literature often describes coacervates as microphase separated, evidenced by scattering or opacity. Certain elements of simplicity benefit the system studied here: the polyelectrolytes are fully charged, not sensitive to pH and bear only one type of charged repeat unit (as opposed to biological molecules). Up to $PEC_{1.70}$, each temperature defines an equilibrium composition, meaning any temperature change leads to microphase separation followed by gradual coalescence of the microphase into one of the two macrophases.[42]

Composition. The equilibrium composition (polymer, salt, water) at room temperature of PSS/PDADMA PEC was carefully determined over a wide range of salt concentrations. Initially, measurements were split between lower KBr concentrations where the PEC was stiff but elastic (i.e., clearly a PECOX) and higher [KBr], where the PEC was soft and eventually clearly a PECOV. An example of PEC doping for [KBr] < 0.6 M is shown in Figure 5a. The salt concentration inside the PEC, given as a mole ratio of KBr to PSS/PDADMA ion pairs ($[C_8H_7SO_3]^-[C_8H_{16}N]^+$ molecular weight 309.42 g mol^{-1}), is linearly dependent on salt concentration outside the PEC, as found previously for other salts.[34] Over this range of salt concentrations each KBr breaks one polymer/polymer ion pair and the counterion is specifically associated with the polyelectrolyte repeat unit, as in eq 1. The fact that the plot almost goes through the origin shows no residual KBr is left in the complex immersed in pure water. If y is the fraction of ion pairs broken by doping (the "doping level"), the fit in Figure 5a is

$$y = 0.5619[KBr] - 0.0094 \quad (r^2 = 0.9964) \qquad (3)$$

Pressing the [KBr] to higher concentrations than 0.6 M (Figure 5b) leads to a nonlinear increase in the KBr/PE ratio. The solution/coacervate phase volume ratio increases as in Figure 1, although there is no clearly observed transition until the two phases disappear at about 1.80 M KBr, where the complex is presumed to dissolve to give a homogeneous solution (supported by additional measurements presented below).

Quantitative NMR spectroscopy, providing the amount and ratio of each polyelectrolyte, shows the following (Figure 6):

(1) There is no measurable polyelectrolyte in the dilute phase for low [KBr] (PECOX), whereas for PECOV there is increasing polymer in the dilute phase, as the polymer concentration in the concentrated phase decreases. PE concentration in the dilute and concentrated phases converge at the dissolution point.

(2) The ratio of PSS to PDADMA remains 1:1 in the PECOX regime but divergence is seen in the PECOV. The concentrated phase becomes slightly richer in PSS and the dilute phase has significantly more PDADMA than PSS. Of course, in the solution state the ratio of PSS:PDADMA returns to 1.0, since this was the initial ratio added in the starting complex.

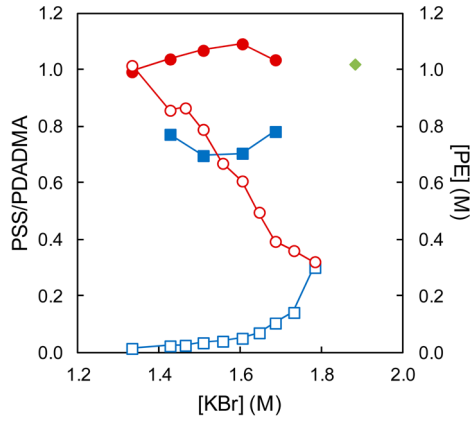

Figure 6. Molar ratio of PSS/PDADMA (solid symbols) and [PE] (open symbols) in dilute (blue squares) and coacervate (red circles) phases by ^1H NMR. Green diamond shows the ratio of PSS/PDADMA in the (uniform) solution.

A significant point is reached when y = 1.00, where all ion pairs are broken and the PEC becomes a solution of isolated, dissolved polyelectrolyte chains. From the extrapolation of the data in Figure 5a (i.e., eq 2) this point would be at [KBr] = 1.80 M. At any y < 1.00, the chains interact through ion pairing (i.e., there exists a PEC of some morphology).

Convergence of polymer concentrations in the two phases at the dissolution point is consistent with thermodynamic control of composition. The excess PDADMA in the dilute PECOV phase may indicate that concentrated KBr is a better solvent for PDADMA(Br) than for PSS(K).

Data on all PEC compositions in weight% is combined into the phase diagram in Figure 7. Details of this phase diagram are consistent with PSS/PDADMA behavior previously re-

dx.doi.org/10.1021/ma500500q | Macromolecules 2014, 47, 3108−3116

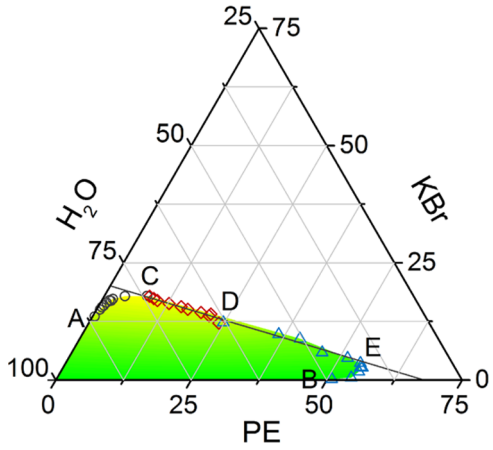

Figure 7. Ternary phase diagram for equilibrium compositions in weight% PSS/PDADMA PE, KBr and water in the dilute phase (○), coacervate phase (◇), and PECOX (Δ). The solid line is a fit of H_2O wt % vs KBr wt % for PE rich phases (PECOX and coacervate): H_2O % = 2.38 KBr % + 32 (r^2 = 0.958). This line crosses the PE % axis at PE % = 68%, which means there are eight water molecules incorporated with each PSS/PDADMA pair.

ported.[28,43] For example, as the % KBr → 0 the complex expands slightly (points E to B), also seen for doping PSS/PDADMA with NaCl.[28] Points B, E, and D define PECOX. Coacervate exists over a relatively narrow %KBr range from D to C. The PE concentration of the dilute phase starting from A converges with the PE concentration in the coacervate at point C.

Boundary between Complex and Coacervate. Figure 5b shows a gradual change in composition of PEC over the entire range of [KBr]. When the PEC is tough and elastic at lower doping levels, the sample would be considered to be in the PECOX regime. At the higher [KBr], particularly in a narrow band of [KBr] between about 1.5 M and the dissolution point (about 1.8 M KBr) the PEC behaves more like a fluid and could reasonably be labeled a PECOV. There is a wide range of [KBr], from about 0.6 M to about 1.6 M (Figure 5b), where the amount of salt entering the PEC is a nonlinear function of the solution [KBr]. Can a boundary be defined where complex turns into coacervate with sufficient [KBr]?

The mechanical properties of PECs depend strongly on the level of doping.[35,44,45] Each polymer/polymer ion pair may be viewed as a dynamic physical cross-link. In accordance with classical theories of rubber elasticity, the modulus is related to the cross-link density.[35] We have previously examined modulus as a function of doping in the y < 0.3 regime.[29,35] Here, we focus on higher KBr concentrations giving PECOV response. Figure 8 depicts PEC storage (G') and loss (G'') shear modulus and the viscosity, η, as a function of [KBr]. Below $[KBr]_c$ there is a strong nonlinear decrease in these parameters with added salt. At $[KBr]_c$ (= 1.80 M) the slope of η vs [KBr] changes abruptly (second order transition), and thereafter a slow decrease in η is seen for the polyelectrolyte solution state.

A Newtonian liquid should not have the storage modulus seen in Figure 8 over much of the [KBr] range. G' drops quickly but is still measurable up to about 1.6 M KBr. Because the coacervate remains a network up to 1.80 M KBr, an elastic component to the modulus is expected. There is a distinct point at around 1.3 M KBr where G' and G'' cross, which could be used to define a complex/coacervate boundary. Use of this single condition is somewhat tentative since all the properties

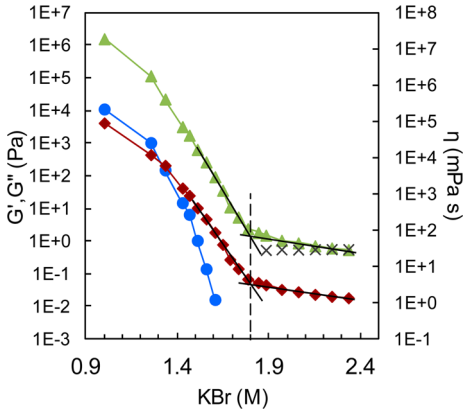

Figure 8. Dynamic modulus G' (●), G'' (▲), and η (■) at 0.1 Hz, shear stress of 25 Pa for PSS/PDADMA with increasing [KBr]. Averages of the viscosities of pure PDADMA and PSS in the appropriate [KBr], representing completely nonion paired chains, are shown as crosses.

and compositions show no clear change in slope. On the other hand, it is less arbitrary than picking a viscosity to define a PECOX/PECOV transition.

Viscosity continues to decrease slightly past 1.8 M KBr (Figure 8), suggesting a few ion pair interactions remain. To simulate a system where no ion pairing is possible, solutions of pure PDADMA and PSS components were prepared in KBr at twice the individual concentrations of those in Figure 8. The viscosities were measured (see Supporting Information), averaged and shown in Figure 8. These nonpairing surrogates yielded average viscosities that were close to those with ion pairing eliminated by KBr addition. The small difference in viscosity between dissolved PEC and the nonpairing surrogates at [KBr] >1.8 M is believed to be a result of a few interactions left over between the longest chains in the former.

Ideally, narrow molecular weight distribution samples should be employed for investigating PEC phases. Such samples are not available for PDADMAC. An estimate $[KBr]_c$ is provided by the following simple approximation:

$$DP = \frac{1}{1-y} = \frac{1}{1-0.56[KBr]_c} \quad (4)$$

Here DP is the degree of polymerization and eq 3 has been approximated by y = 0.56[KBr]. This relationship between $[KBr]_c$ and DP is shown in Figure 9. A molecular weight of

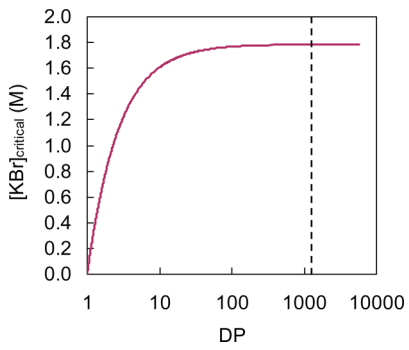

Figure 9. Calculated $[KBr]_{critical}$ for dissolution of PEC as a function of the degree of polymerization, DP, of polyelectrolytes. PSS with molecular weight of 200 000 has a DP (=N) of about 1080, which is shown by the dotted line.

dx.doi.org/10.1021/ma500500q | Macromolecules 2014, 47, 3108−3116

200 000 is a DP of about 1080 for PSS, indicated by the vertical dotted line in Figure 9. In the broad molecular weight distribution sample employed here there are, of course, many much smaller, and a few much longer chains, but $[KBr]_c$ is relatively insensitive to molecular weight above a DP of about 100. Conditioning of a PECOV at $[KBr] < [KBr]_c$ for some time should enrich the higher molecular weight fraction of polymer in the PECOV. We have not tested this interesting possibility.

The Rôle of Salt over the Composition Spectrum. The continuum of PEC salt concentration shown in Figure 5 reveals a linear dependence of KBr/PE for [KBr] < 0.6M, shown in detail in Figure 5a, followed by a long nonlinear portion from 0.6 M to about 1.6 M. From 1.6 M to the dissolution point, salt easily enters the PEC giving a steeper linear KBr/PE slope. What is the salt doing over the 0 to 1.8 M KBr range and where do the ions go? In our current view of the PEC, salt within the complex has one of two rôles: it is either associated specifically with charges on the polyelectrolyte repeat units (here, sulfonate or quaternary ammonium, i.e., Pol^-M^+ or Pol^+A^- from eq 1), or it is unassociated.

Associated and unassociated ions within the PEC are, of course, able to exchange, but a snapshot of all ions within the PEC would show their equilibrium distribution. At any instant, only associated ions break polymer/polymer pairs. Their concentration in the PEC is $[KBr]_{PEC,A}$. As such, associated ions may be considered ion-paired with polyelectrolyte and are here labeled as polyelectrolyte counterions Pol^+A^- and Pol^-M^+.

The dependence of concentration of unassociated KBr, $[KBr]_{PEC,U}$, on solution [KBr] is described by a partition coefficient, K'_{KBr}

$$K'_{KBr} = f[KBr] = \frac{[KBr]_{PEC,U}}{[KBr]} \tag{5}$$

The total [KBr] in the PEC, $[KBr]_{PEC,total} = [KBr]_{PEC,A} + [KBr]_{PEC,U}$. For coacervates, the cartoon in Scheme 1 depicts associated (paired, doping) ions next to polymer chains and unassociated (partitioned) ions in the spaces between.

K'_{KBr} varies across the [KBr] range. Of course, beyond y = 1.00, K'_{KBr} has no meaning since there is only one phase. At low [KBr], i.e., < 0.6 M, unassociated ions are unable to enter the PEC. This is because the ion pairing (cross-linking) density is so high there is insufficient free volume to include extra ions (with their waters of hydration). For the linear region at [KBr] < 0.6 M, K'_{KBr} approaches zero, $[KBr]_{PEC,U} \rightarrow 0$, $[KBr]_{PEC,A} = [Pol^+A^-] = [Pol^-M^+]$ and y = KBr/PE. As cross-links are broken more free volume becomes available so $[KBr]_{PEC,U}$ increases, whereupon y < KBr/PE. Finally, the cross-links become so dilute that they do not restrict the free volume (beyond [KBr] = 1.6 M) and K'_{KBr} becomes constant (see the linear portion from 1.6 to 1.8 M KBr in Figure 5b), approximately unity (see Supporting Information Figure S2).

The scenario above is an example of polymer cooperativity—at low doping levels ion pairs work cooperatively to exclude unassociated KBr from the PEC. The point at which y = 1.00 may be extrapolated from the linear doping data in Figure 5a (i.e., eq 3) to predict $[KBr]_c$ = 1.80. This is the same as the value determined experimentally by either observing the disappearance of the 2 phase regime (Figure 1) or from the viscosity data in Figure 8. Alternatively, one may justify the extrapolation by using the y = 1.00 point and its experimental $[KBr]_c$= 1.80 M.

This labeling of the instantaneous role of counterions within the PEC is somewhat untraditional, as all ions are usually treated equally in mean field approximations. But there is strong historical precedent in the field of classical ion exchangers. These exchangers, or "resins", have fixed polymer charges, often in the form of sulfonates or quaternary ammoniums, and mobile small (counter) ions.[46] The fixed charges generate a Donnan potential which excludes like-charged counterions (co-ions) over a range of solution ion concentration (i.e., they are "selective" for oppositely charged cations or anions). It is known that at sufficiently high salt concentration classical ion exchangers are no longer able to exclude co-ions and neutral salt enters the exchanger.[46] This condition is known as Donnan breakdown.[47]

In the PEC system, which becomes an ion exchanger under the influence of external salt (a so-called "reluctant" exchanger[48]), the deviation from linear KBr/PE at low [KBr] is taken as the start of Donnan breakdown and the entry of unassociated salt. The Donnan breakdown regime is shown in Figure 5b.

Time, temperature and salt in these saloplastic materials are interrelated.[29,44] For example, a higher salt concentration lowers the glass transition temperature, T_g.[29] According to prior work on PSS/PDADMA complex doped with NaCl, a T_g at 20 °C and 0.1 Hz is seen at around 0.69 M NaCl and y = 0.25.[29] This corresponds to about 0.46 M KBr from Figure 5a. At lower [KBr] the PEC is glassy. The transition from glassy to rubbery is also shown in Figure 5b. We have placed this transition at y = 0.25, i.e., where 1/4 of ion pairs have been broken, because we believe the starting point for the loss in cooperativity (Donnan breakdown) is *also* fundamentally responsible for the glass transition.[49] The glass transition is broad and all of the boundaries, except the transition to the dissolved state, in Figure 5b should be viewed as diffuse.

Using the doping curve to estimate the fraction of ion pairing allows us to analyze the coacervate viscosity using the "sticky reptation" theory of Rubinstein and Semenov.[50] According to this theory, polymer chains in solution are above their overlap concentration and experience transient entanglements impeding their reptating motion. The critical volume fraction for chain overlap,[51] φ^*, is about $N^{1/2}$ where N is between about 1000 and 3000 depending on whether the PSS or the PDADMA fraction is used for this estimate, which gives a φ^* between 2 and 3%, lower than the experimental volume fractions (Figure S3). Favorable interactions between oppositely charged chains encourage entanglements and blending at a molecular level.[52] A steady state number, f, of repeat units in a chain, separated by l unassociated units, experience specific "sticky" interactions (here, polyelectrolyte ion pairing), associating physically with association lifetime τ_b. For conditions where the polymer strands are entangled between stickers and Θ-conditions (assumed to be approximated here because of the high salt concentration), the viscosity is given by

$$\eta \approx \frac{kT\tau_b}{b^3 {N_{e0}}^2} e^{\varepsilon/2} f^3 \left(\frac{l}{N_{e0}}\right)^{3/4} \varphi^{25/6} \tag{6}$$

where k is Boltzmann's constant, T is the temperature, b is the monomer size, N_{e0} is the number of monomers between entanglements in a melt (i.e., pure PEC with no water or salt), ε is the sticker binding energy (ion pairing energy), and φ the polymer volume fraction. Other boundary conditions are $f \gg 1$ and $l \gg 1$. In our system, τ_b is unknown but assumed to be

dx.doi.org/10.1021/ma500500q | Macromolecules 2014, 47, 3108−3116

inversely proportional to salt concentration (i.e., $\tau_b \sim 1/y$) and ε, also unknown, is assumed constant. Our doping terminology conveniently means $f \sim 1 - y$ and $l = y/(1 - y)$. Thus, the appropriate scaling is

$$\eta = \frac{k}{y}(1 - y)^3\left(\frac{y}{1 - y}\right)^{3/4}\varphi^{25/6} \quad (7)$$

where k is a scaling constant. Volume fractions of PE were estimated from the composition data assuming respective densities for PE, KBr and water of 1.13, 2.75, and 1.00 g mL^{-1}. The volume fraction of PE (φ_{PE}) fit the equation $\varphi_{PE} = 0.679(1 - y) + 0.075$ ($r^2 = 0.9708$) (see Supporting Information, Figure S3).

Using doping eq 3 to correlate [KBr] in Figure 8 to $1 - y$, viscosity, with the slight ramp from the dissolved PE regime subtracted, is plotted against 1-y in Figure 10. Here, $1 - y$ is the fraction of polyelectrolyte that is associated (fraction of stickers). Equation 7 is plotted with a scaling constant of 3.18×10^9. Reasonably good agreement between data and fit is seen except for the lowest viscosity range when the PEC is almost dissolved (due to incomplete background subtraction). Points at $1 - y < 0.2$ were used to optimize the fit ($r^2 = 0.998$). We were surprised to see agreement extend to higher $1 - y$ where the assumption $l \gg 1$ breaks down.

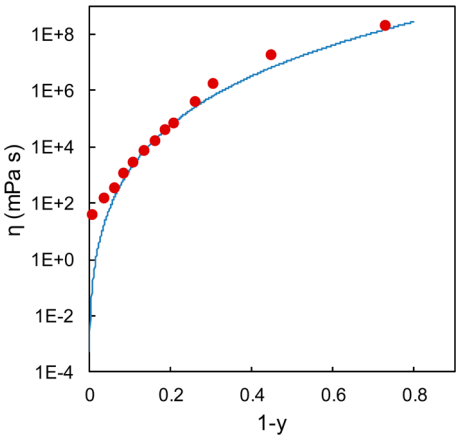

Figure 10. Fitted (blue line) and experimental (red symbols) viscosity of cross-linked strands with entanglement between the stickers vs the pairing fraction.

Spruijt et al. have recently provided a "sticky Rouse" model for coacervate complex viscosity, where entanglement is not featured.[53] Their model would drastically underpredict our observed dependence of viscosity with salt concentration (4 orders of magnitude change in η for a 30% change in salt concentration). Their model also underestimates their own data on dependence of viscosity on salt concentration.

CONCLUSIONS

Glassy, rubbery, and liquid forms of polyelectrolyte complexes in aqueous environments are interconnected by salt concentration. A "backwards" method of dissolving, and then reprecipitating, complexes yielded what are believed to be equilibrium compositions. The equilibrium nature of the coacervate state was established but the polyelectrolyte composition of PECOX is only believed to be an equilibrium composition because the preparation method gives stoichiometric polyelectrolytes. In contrast, sorption of ions into PEC of any form is known to be in equilibrium with solution ions. By extrapolating the linear doping behavior at low salt concentration it was clearly shown that complexes in all morphologies are held together by polyelectrolyte/polyelectrolyte ion pairing. The doping relationship predicts the extent of ion pairing with salt concentration, which was used to model the viscosity of PECs (beyond the glass transition) using a model of "sticky" reptation.

ASSOCIATED CONTENT

Supporting Information

Coacervate samples prepared by the "forward" method, video of microphase separation, KBr concentration in dilute and uniform phases, volume fraction of polyelectrolyte as a function of KBr concentration, and viscosities of single polyelectrolytes in KBr. This material is available free of charge via the Internet at http://pubs.acs.org.

AUTHOR INFORMATION

Corresponding Author

*(J.B.S.) E-mail schlen@chem.fsu.edu.

Notes

The authors declare no competing financial interest.

ACKNOWLEDGMENTS

We thank Carlos Arias Ramos for the NMR measurements and analysis. This work was supported by Grant DMR 1207188 from the National Science Foundation.

REFERENCES

(1) Bixler, H. J.; Michaels, A. S. Polyelectrolyte complexes. *Encycl. Polym. Sci. Technol.* **1969**, *10*, 765−780.
(2) Michaels, A. S. *Ind. Eng. Chem. Res.* **1965**, *57* (10), 32−40.
(3) Turgeon, S. L.; Schmitt, C.; Sanchez, C. *Curr. Opin. Colloid Interface Sci.* **2007**, *12* (4−5), 166−178.
(4) Hwang, D. S.; Zeng, H.; Srivastava, A.; Krogstad, D. V.; Tirrell, M.; Israelachvili, J. N.; Waite, J. H. *Soft Matter* **2010**, *6* (14), 3232−3236.
(5) Porcel, C. H.; Schlenoff, J. B. *Biomacromolecules* **2009**, *10* (11), 2968−2975.
(6) Philipp, B.; Dautzenberg, H.; Linow, K.-J.; Kötz, J.; Dawydoff, W. *Prog. Polym. Sci.* **1989**, *14* (1), 91−172.
(7) Dautzenberg, H. *Macromolecules* **1997**, *30* (25), 7810−7815.
(8) Tsuchida, E.; Osada, Y.; Ohno, H. *J. Macromol. Sci. Phys.* **1980**, *B17* (4), 683−714.
(9) Oyama, H. T.; Frank, C. W. *J. Polym. Sci., Part B: Polym. Phys.* **1986**, *24* (8), 1813−1821.
(10) Schmitt, C.; Sanchez, C.; Desobry-Banon, S.; Hardy, J. *Crit. Rev. Food Sci. Nut.* **1998**, *38* (8), 689−753.
(11) Kizilay, E.; Kayitmazer, A. B.; Dubin, P. L. *Adv. Colloid Interface Sci.* **2011**, *167* (1−2), 24−37.
(12) Chollakup, R.; Beck, J. B.; Dirnberger, K.; Tirrell, M.; Eisenbach, C. D. *Macromolecules* **2013**, *46* (6), 2376−2390.
(13) Michaeli, I.; Overbeek, J. T. G.; Voorn, M. J. *J. Polym. Sci.* **1957**, *23* (103), 443−450.
(14) Overbeek, J. T. G.; Voorn, M. J. *J. Cell. Comp. Physiol.* **1957**, *49* (S1), 7−26.
(15) Khokhlov, A. R.; Nyrkova, I. A. *Macromolecules* **1992**, *25* (5), 1493−1502.
(16) Bungenberg de Jong, H. G.; Kruyt, H. R. *Proc. Sect. Sci. K. Ned. Akad. Wetenschappen* **1929**, *32*, 849−856.
(17) Stewart, R. J.; Weaver, J. C.; Morse, D. E.; Waite, J. H. *J. Exp. Biol.* **2004**, *207* (26), 4727−4734.

(18) Shao, H.; Bachus, K. N.; Stewart, R. J. *Macromol. Biosci.* **2009**, *9* (5), 464−471.
(19) Hwang, D. S.; Waite, J. H.; Tirrell, M. *Biomaterials* **2010**, *31* (6), 1080−1084.
(20) Koga, S.; Williams, D. S.; Perriman, A. W.; Mann, S. *Nat. Chem.* **2011**, *3* (9), 720−724.
(21) Huang, X.; Li, M.; Green, D. C.; Williams, D. S.; Patil, A. J.; Mann, S. *Nat. Commun.* **2013**, *4*, 1−9.
(22) Oh, Y. J.; Cho, I. H.; Lee, H.; Park, K.-J.; Lee, H.; Park, S. Y. *Chem. Commun.* **2012**, *48* (97), 11895−11897.
(23) Fuoss, R. M.; Sadek, H. *Science* **1949**, *110* (2865), 552−554.
(24) Michaels, A. S.; Miekka, R. G. *J. Phys. Chem.* **1961**, *65* (10), 1765−1773.
(25) Decher, G. *Science* **1997**, *277* (5330), 1232−1237.
(26) Decher, G.; Schlenoff, J. *Multilayer Thin Films: Sequential Assembly of Nanocomposite Materials*, 2nd ed.; Wiley-VCH: Weinheim, Germany, 2012.
(27) Sukhishvili, S. A.; Kharlampieva, E.; Izumrudov, V. *Macromolecules* **2006**, *39* (26), 8873−8881.
(28) Shamoun, R. F.; Reisch, A.; Schlenoff, J. B. *Adv. Funct. Mater.* **2012**, *22* (9), 1923−1931.
(29) Shamoun, R. F.; Hariri, H. H.; Ghostine, R. A.; Schlenoff, J. B. *Macromolecules* **2012**, *45* (24), 9759−9767.
(30) Kayitmazer, A. B.; Seeman, D.; Minsky, B. B.; Dubin, P. L.; Xu, Y. *Soft Matter* **2013**, *9* (9), 2553−2583.
(31) Priftis, D.; Tirrell, M. *Soft Matter* **2012**, *8* (36), 9396−9405.
(32) Park, J. M.; Muhoberac, B. B.; Dubin, P. L.; Xia, J. L. *Macromolecules* **1992**, *25* (1), 290−295.
(33) Farhat, T. R.; Schlenoff, J. B. *J. Am. Chem. Soc.* **2003**, *125* (15), 4627−4636.
(34) Schlenoff, J. B.; Rmaile, A. H.; Bucur, C. B. *J. Am. Chem. Soc.* **2008**, *130* (41), 13589−13597.
(35) Jaber, J. A.; Schlenoff, J. B. *J. Am. Chem. Soc.* **2006**, *128* (9), 2940−2947.
(36) Dautzenberg, H.; Karibyants, N. *Macromol. Chem. Phys.* **1999**, *200* (1), 118−125.
(37) Dautzenberg, H.; Kriz, J. *Langmuir* **2003**, *19* (13), 5204−5211.
(38) Spruijt, E.; Westphal, A. H.; Borst, J. W.; Cohen Stuart, M. A.; van der Gucht, J. *Macromolecules* **2010**, *43* (15), 6476−6484.
(39) Ghostine, R. A.; Shamoun, R. F.; Schlenoff, J. B. *Macromolecules* **2013**, *46* (10), 4089−4094.
(40) Hariri, H. H.; Lehaf, A. M.; Schlenoff, J. B. *Macromolecules* **2012**, *45* (23), 9364−9372.
(41) Salomäki, M.; Tervasmäki, P.; Areva, S.; Kankare, J. *Langmuir* **2004**, *20* (9), 3679−3683.
(42) Spruijt, E.; Sprakel, J.; Cohen Stuart, M. A.; van der Gucht, J. *Soft Matter* **2010**, *6* (1), 172−178.
(43) Dubas, S. T.; Schlenoff, J. B. *Langmuir* **2001**, *17* (25), 7725−7727.
(44) Spruijt, E.; Sprakel, J.; Lemmers, M.; Stuart, M. A. C.; van der Gucht, J. *Phys. Rev. Lett.* **2010**, *105* (20), 208301.
(45) Priftis, D.; Megley, K.; Laugel, N.; Tirrell, M. *J. Colloid Interface Sci.* **2013**, *398* (0), 39−50.
(46) Helfferich, F. G. *Ion Exchange*; McGraw-Hill: New York, 1962.
(47) Calvo, E. J.; Wolosiuk, A. *J. Am. Chem. Soc.* **2002**, *124* (28), 8490−8497.
(48) Farhat, T. R.; Schlenoff, J. B. *Langmuir* **2001**, *17* (4), 1184−1192.
(49) Bauer, T.; Lunkenheimer, P.; Loidl, A. *Phys. Rev. Lett.* **2013**, *111* (22), 225702.
(50) Rubinstein, M.; Semenov, A. N. *Macromolecules* **2001**, *34* (4), 1058−1068.
(51) Rubinstein, M.; Colby, R. H. *Polymer Physics*; Oxford University Press: New York, 2003.
(52) Markarian, M. Z.; Hariri, H. H.; Reisch, A.; Urban, V. S.; Schlenoff, J. B. *Macromolecules* **2011**, *45* (2), 1016−1024.
(53) Spruijt, E.; Cohen Stuart, M. A.; van der Gucht, J. *Macromolecules* **2013**, *46* (4), 1633−1641.